Semiannual Technical Summary

Seismic Discrimination

31 December 1968

Prepared for the Advanced Research Projects Agency
under Electronic Systems Division Contract AF 19(628)-5167 by

Lincoln Laboratory

MASSACHUSETTS INSTITUTE OF TECHNOLOGY

Lexington, Massachusetts

The work reported in this document was performed at Lincoln Laboratory, a center for research operated by Massachusetts Institute of Technology. This research is a part of Project Vela Uniform, which is sponsored by the U.S. Advanced Research Projects Agency of the Department of Defense; it is supported by ARPA under Air Force Contract AF 19(628)-5167 (ARPA Order 512).

MASSACHUSETTS INSTITUTE OF TECHNOLOGY
LINCOLN LABORATORY

SEISMIC DISCRIMINATION

SEMIANNUAL TECHNICAL SUMMARY REPORT
TO THE
ADVANCED RESEARCH PROJECTS AGENCY

1 JULY – 31 DECEMBER 1968

ISSUED 23 JANUARY 1969

LEXINGTON MASSACHUSETTS

ABSTRACT

Seismic source identification work during this reporting period has emphasized improving the ability of short-period discriminants to work at lower magnitudes, and the use of a wider variety of stations, including especially the NORSAR site in Scandinavia. During this period, plans to upgrade our signal analysis capability and at the same time move into closer proximity to the academic part of M.I.T. have reached partial fruition.

Accepted for the Air Force
Franklin C. Hudson
Chief, Lincoln Laboratory Office

CONTENTS

	Abstract	iii
	Summary	vii
	Glossary	viii
I.	IDENTIFICATION	1
	A. New LASA Large-Population Experiment	1
	B. Improvements in Short-Period Spectral Discriminants	5
	C. Application of Multivariate Classification Methods	11
	D. Velocity Spectral Analysis (VESPA) of P-coda	13
	E. Teleseismic Coda Generation by Scattering of Rayleigh Waves	17
	F. Surface Wave Discrimination at NORSAR	19
II.	MULTISITE EXPERIMENTS	21
	A. Data Library	21
	B. Continental Arrays	21
III.	ARRAY STUDIES	23
	A. Large Array Epicenter Location Using High-Resolution Frequency-Wavenumber Analysis	23
	B. Direction of Approach of Rayleigh Waves	23
	C. Short-Period Noise Analysis Using High-Resolution Mapping	24
IV.	MISCELLANEOUS	31
	A. Physical Facilities	31
	B. Calculated Seismic Magnitude of Missile Launches	31

SUMMARY

This is the tenth Semiannual Technical Summary of Lincoln Laboratory's work for the Advanced Research Projects Agency on the seismic discrimination problem (Vela Uniform).

A large data base of parameter measurements on many earthquakes and presumed explosions has been generated and subjected to previously available explosion-earthquake discriminants, such as long-period surface wave and short-period spectral ratio measurements (Sec. I-A). By using this data base, several parallel efforts to improve short-period discrimination beyond that available from spectral ratio alone have been made recently. These approaches, which have offered a modest improvement in decreasing the short-period identification threshold, are described in Secs. I-B and -C and involve the use of dominant period, detailed examination of spectral behavior as a function of source type and magnitude, and application of pattern classification algorithms.

In an attempt to understand the use of P complexity (ratio of P-coda to P) as a source discriminant, detailed directional analysis of several events has shown that the coda has the same direction of approach as P, within the resolving power of the LASA (Sec. I-D). A possible explanation of the high complexity values from certain regions is offered in Sec. I-E.

Use of data from the initial NORSAR installation has been extended to surface wave discrimination studies. The observed different behavior of the western U.S. and Central Asia areas has suggested an attempted explanation in terms of basic differences in tectonic type of the two regions (Sec. I-F).

A data base is being prepared for joint use of data from LASA, NORSAR, and other stations to simulate a net of mixed station types (Sec. II-A). The combined use of single-sensor stations distributed over a several-thousand kilometer aperture (continental array) is being studied for improved depth phase and P-coda analysis (Sec. II-B).

Investigations using high-resolution wavenumber mapping are now substantially complete, having been extended to short-period noise, long-period signal, and epicenter location problems (Sec. III).

Recent changes in our physical facilities, involving a move to closer proximity to the Department of Geology and Geophysics at M.I.T. and improvements in processing hardware and software, are reported in Sec. IV-A.

Section IV-B attempts to settle quantitatively a recurring question concerning seismic detectability of missile launches.

P. E. Green

GLOSSARY

ARPA	Advanced Research Projects Agency
LASA	Large Aperture Seismic Array
LP	Long-Period
LRSM	Long Range Seismic Measurements
NORSAR	Norwegian Seismic Array
SATSR	Semiannual Technical Summary Report
SNR	Signal-to-Noise Ratio
SP	Short-Period
TFO	Tonto Forest Observatory
USCGS	United States Coast and Geodetic Survey
VESPA	Velocity Spectral Analysis

SEISMIC DISCRIMINATION

I. IDENTIFICATION

A. NEW LASA LARGE-POPULATION EXPERIMENT

A total of 197 events recorded by LASA have been processed to generate a data base for discrimination studies. All but 28 of these events were either presumed underground nuclear explosions at teleseismic distances from LASA, or earthquakes within or close to Sino-Soviet areas. The computer programs and procedures were briefly described in our previous Semi-annual Technical Summary Report (SATSR).[1]

Each of the events has been inspected for possible depth phases and the depths implied by these phases compared with USCGS depths whenever possible. LASA reported probably pP picks for 55 of the 87 earthquakes in our data base which were reported by USCGS. Exclusivc of events which USCGS restricted to 33 km, LASA and USCGS depths agreed to within 25 percent for 65 percent of the common events. Agreement is almost perfect for depths greater than 100 km.

Two distinct methods have been used to give a new estimate of the probability of detecting surface waves at LASA as a function of body wave magnitude (m_b). First, all earthquakes with available LP recordings and without interference from other events were studied. Figure I-1 shows the percent of events having detected surface waves as a function of LASA body wave magnitude. Percentages were computed using events within body wave magnitude intervals 0.1 magnitude units wide. The computation did not include any events at depths more than 100 km. The dashed line on the figure can be considered as the nominal probability of surface wave detection for earthquakes. A second approach, based primarily upon the amplitude distribution of background noise, has also been used to estimate the probability of surface wave detection. In general, all data have indicated that the surfacc wave detection probability for shallow events is above 50 percent for $m_b \geqslant 4.5$ and is about 100 percent for $m_b \geqslant 4.8$.

The relative excitation of surface and body waves by earthquakes and explosions as measured at LASA has been previously established as a powerful discriminant. Figure I-2 shows the $M_s - m_b$ data for our latest large-population experiment. Separation between earthquakes and explosions is excellent but, unlike earlier results, not perfect. One earthquake (latitude 48.2 N, longitude 157.3 E, origin time 16:04:37.9, 23 Dccember 1967) is surrounded by explosion points. If the points on Fig. I-2 which have been reported by USCGS are replotted vs the USCGS m_b, thc separation becomes complete, although the problem earthquake remains quite close to the explosion points. The radiation pattern for the problem event may have caused LASA to measure an anomalously high m_b or anomalously low M_s, or both.

Figure I-3 is a plot of spectral ratio vs magnitude. The two trend lines and the decision line, which is their geometric mean, are exponentials. Only a few events would be incorrectly identified by the decision line shown. If all earthquakes with observed pP are removed, then only low-magnitude explosions remain on the wrong side of the decision line.

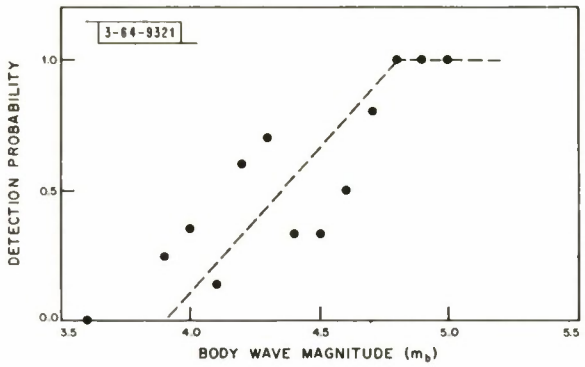

Fig. I-1. LASA surface wave detection prabability vs magnitude far narmal depth earthquakes (winter conditians).

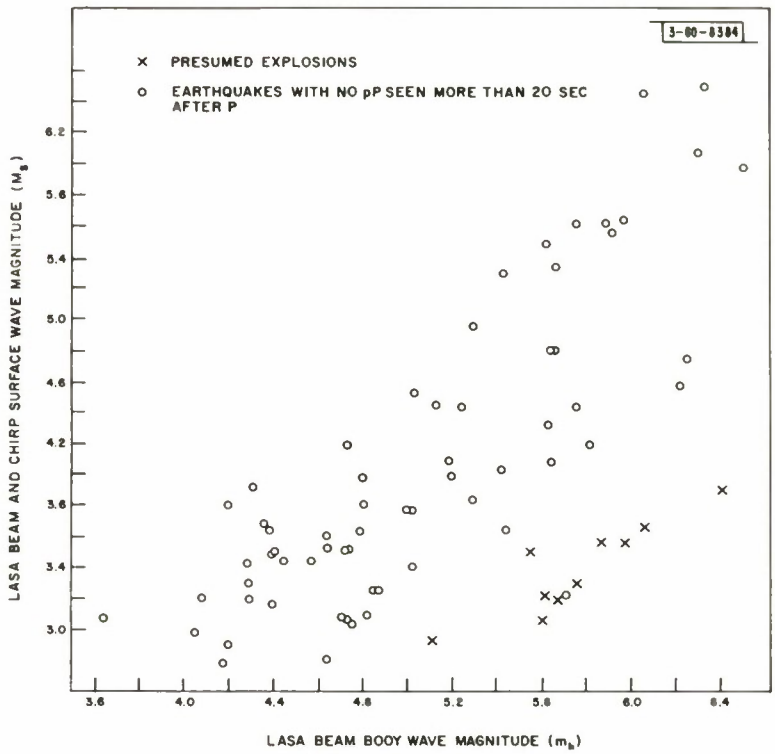

Fig. I-2. Discriminatian using LASA surface wave vs body wave magnitude.

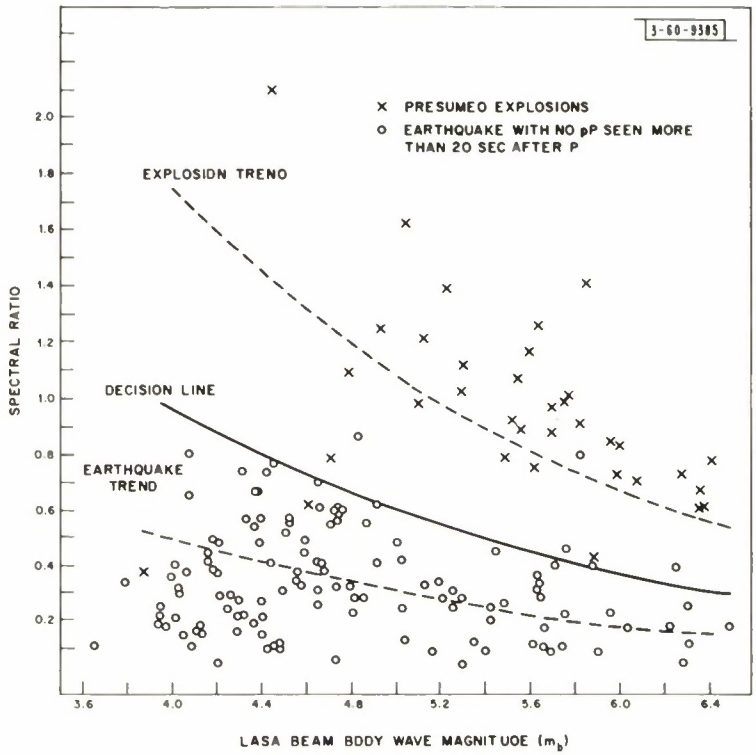

Fig. I-3. Discrimination using LASA short-period spectral ratio.

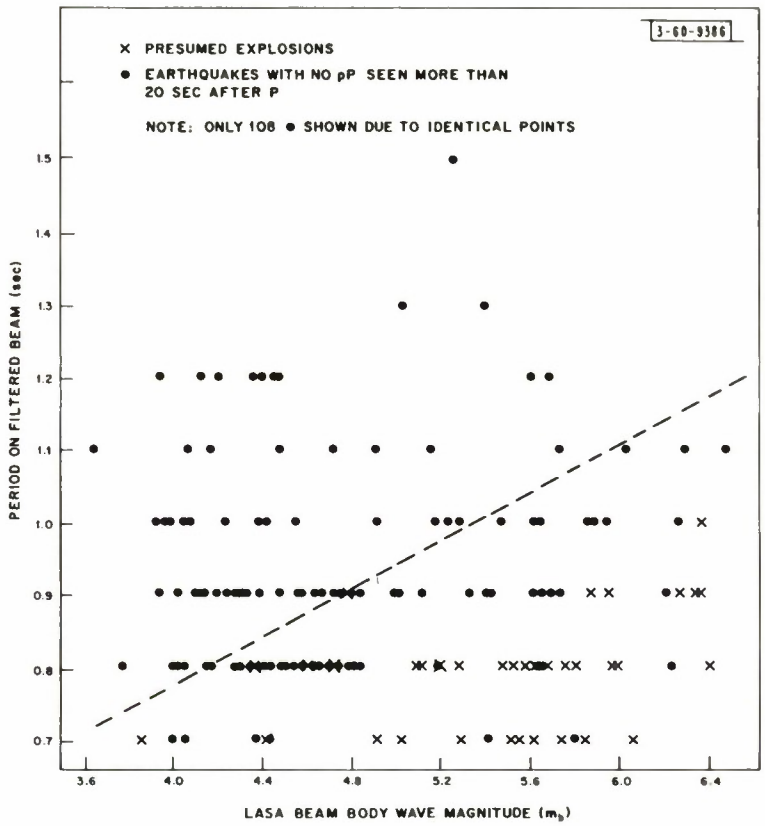

Fig. I-4. Discriminotion using LASA P-dominant period.

Both the operational aspects and the discrimination analysis will be discussed in detail in a forthcoming report.

R. T. Lacoss

B. IMPROVEMENTS IN SHORT-PERIOD SPECTRAL DISCRIMINANTS

It has long been recognized that spectral ratio can be severely affected by a poor signal-to-noise ratio. This has now been investigated in some detail and, as a result, a modification of the spectral ratio criterion has evolved which specifies that no decision be made in some cases. Let V_B be the integral from 0.35 to 0.85 Hz of the measured voltage spectrum of an event, and V_H be a similar integral from 0.45 to 0.95 Hz. Spectral ratio, which is defined as $\rho = V_H/V_L$, is thus influenced by background noise contributions to V_H and V_L. Let ${}_NV_H$ and ${}_NV_L$ be the same measurements as V_H and V_L but made on noise immediately preceding the event. (The values of ${}_NV_H$ and ${}_NV_L$ may be averages over two or more noise intervals preceding the event.) Define $\rho_H = V_H/{}_NV_H$ and $\rho_L = V_L/{}_NV_L$. The modified decision rules which depend on ρ_H, ρ_L, as well as ρ and m_b, are as follows:

$\rho_H > 3$, $\rho_L > 3$	Accept spectral ratio measurement ρ, and discriminate according to the decision line shown on Fig. I-3.
$\rho_H > 3$, $\rho_L < 3$	If ρ indicates explosion, then decide explosion. If ρ indicates earthquake, make no decision.
$\rho_H < 3$, $\rho_L > 3$	If ρ indicates earthquake, then decide earthquake. If ρ indicates explosion, make no decision.
$\rho_H < 3$, $\rho_L < 3$	Make no decision.

The modified decision rule is designed to make effective use of spectral data without being misled by strictly noise effects. Using this rule on the data of Fig. I-3, no explosions were misidentified as earthquakes since all explosions in the earthquake region had $\rho_L < 3$. Simultaneously, the modified rule correctly identified all other explosions. It is estimated that the probability of making any decision is about unity near $m_b = 4.5$ and drops to zero at about $m_b = 4.1$.

Figure I-4 shows a plot of dominant period vs LASA m_b for events in our data base. These data are an improved version of those presented previously by Kelly,[2] involving a greater number of events and measurements by computer rather than by an analyst. A possible decision line has been drawn on the figure which contains all explosions in the lower right section. The plot suggests that all explosions, even down to below magnitude 4.0, can be identified using period but that only 53 percent of earthquakes are correctly identified. However, in the important range below $m_b = 4.5$, about 72 percent of the earthquakes are correctly identified. Although period can clearly not be a perfect discriminant, it becomes increasingly powerful at low magnitudes where $M_s - m_b$ and spectral ratio become almost useless.

R. T. Lacoss

One of the outputs of the analysis program described in the preceding section is the amplitude spectrum of each processed event, which is saved on magnetic tape, together with magnitude m_b and other parameters. We have used the spectra for presumed explosions and earthquakes as the

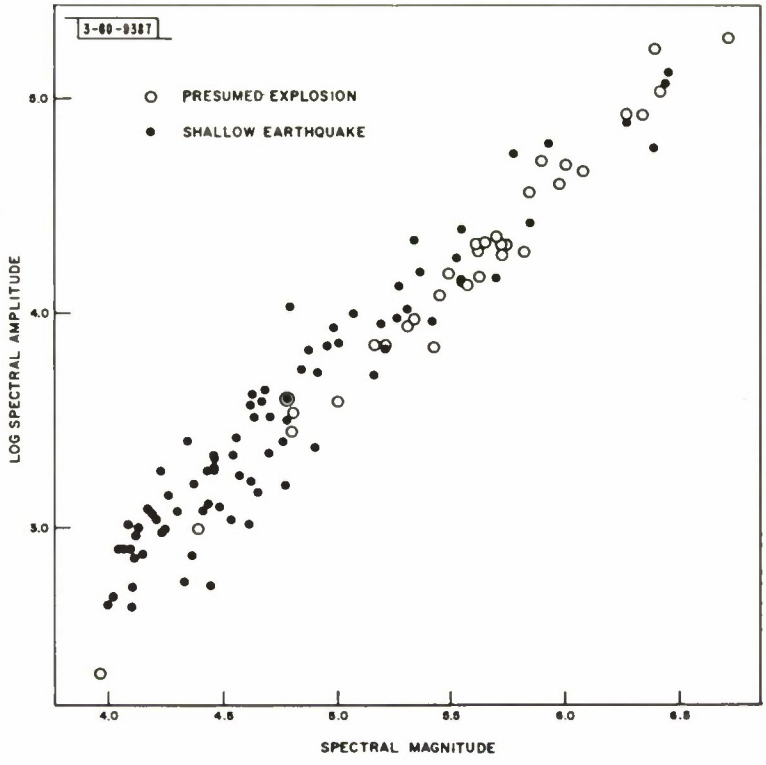

Fig. I-5. Logorithm of amplitude at 1.0 Hz vs body wove mognitude.

starting data basc for a new study whose two main objectives are: (1) to find the optimum short-pcriod spectral discriminant, and (2) to obtain experimental data on the source spectra of cx-plosions and earthquakes avcraged over relatively large populations, and to compare the results with recent theoretical work on average spectra.[3,4]

The recorded spectra are first subjected to some processing which is common to both lines of study, and this will be briefly described first. The current status of the work in the two main directions will then be summarized. It can be stated at this point, however, that the best spec-tral discriminants found so far are only slightly superior to the original spectral ratio tcchnique, although the procedure used to find them should prove useful with data from other sites.

The original spectra are formed by extending the 200 data samples (10 sec worth) to 2048 samples by adding zeros, and then computing the absolute values of the first 1025 discrete Fourier transform coefficients (i.c., zero frequency to the Nyquist frequency). We have smoothed these spectra to produce spectral energy densities at each multiple of 0.1 Hz, from 0.1 to 3.0 Hz, by averaging the squares of the original spectral amplitudes over 0.1-Hz wide bands centered at the desired frequencies. We then take one-half the logarithm of the energy density to obtain a log spectral amplitude, and all further work is based upon these thirty numbers for each event.

We are interested in the spectra as functions of both frequency and magnitudc. By display-ing the log spectral amplitude at a fixed frequency, for each event vs its body wave magnitude, we obtain a scatter diagram such as that shown in Fig. I-5 for a frequency of 1.0 Hz. We define two populations: presumed explosions and shallow earthquakes, i.e., having no detected pP arriving more than 10 sec after P. For each population, and at each frequency, the log spectral amplitude vs magnitude data are least-squares fitted with a straight line. This results in "av-erage" spectra of the form

$$S(f) = A(f)\, m_b + B(f) \qquad (I\text{-}1)$$

(where S stands for log spectral amplitude, m_b is body wave magnitude, and f is one of the thirty frequencies), and we obtain a pair of functions [A(f), B(f)] for each of the two populations.

Seeking to reduce the scatter, some of which is certainly due to the variability of the orig-inal magnitude measurements in the time domain, we used the average spectra to redetermine a "spectral magnitude" for each event. This was done by fitting the measured spectrum of each event, over the frequency range $0.7 \leqslant f \leqslant 2.4$ Hz (outside this band we begin to lose adequate signal-to-noise ratio for the weaker events), to the appropriate formula [Eq. (I-1)], and then using least squares to determine the m_b parameter. The resulting spectral magnitudes are not greatly dif-ferent from the time-domain values. We then iterated the whole procedure, displaying log spec-tral amplitude vs the new spectral magnitude and determining new straight-line parameters A(f) and B(f). The residuals to these straight-line fits were significantly reduced by this iteration, but the "average spectra" obtained were changed very little. In the solid lines of Fig. I-6, we show a plot of the average explosion spectra, computed from Eq. (I-1), for values of spectral magnitude of 4.5, 5.5, and 6.5. A corresponding set derived from the earthquakes is shown as dashed lines. The difference of these log-amplitude spectra, for spectral magnitude 5.5 (bomb minus quake) is shown also.

In order to study source spectra, we have first removed the LASA system response from the average spectra, which results in log-amplitude plots which decrease roughly linearly with

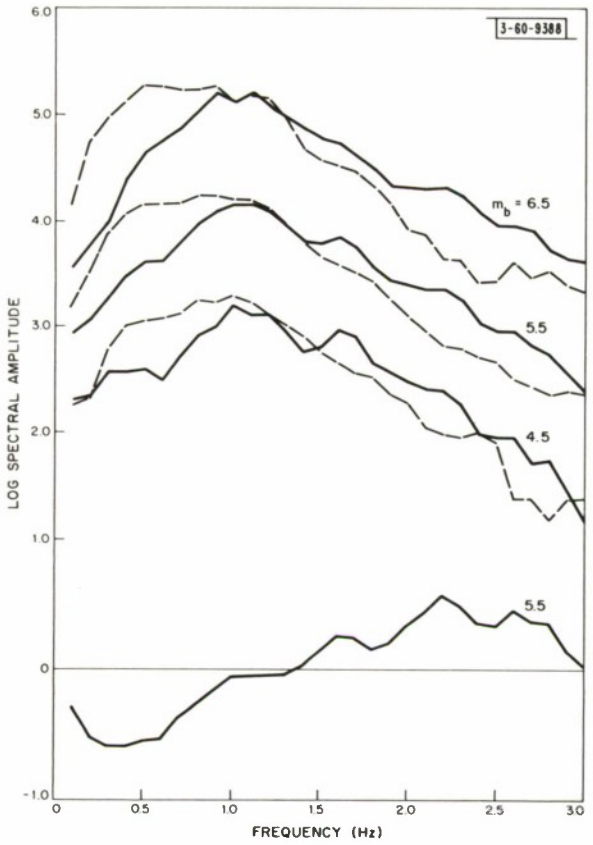

Fig. I-6. Averaged spectra at three spectral magnitudes for presumed explosions (solid lines) and shallow earthquakes (dashed lines). The difference for spectral magnitude 5.5 is shown at bottom of figure.

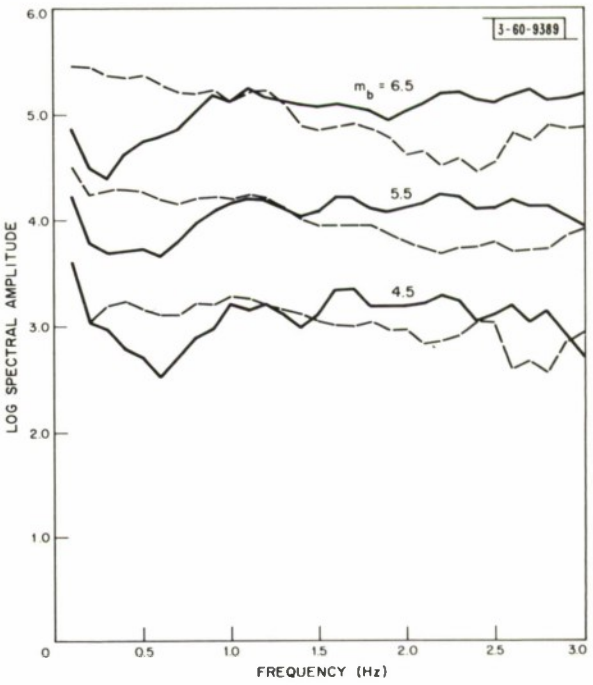

Fig. I-7. Data of Fig. I-6 corrected for characteristics of seismometer and transmission medium.

frequency as expected from the normal attenuation of P-waves in the crust and mantle with a frequency-independent Q. We have arbitrarily chosen a straight line, representing attenuation, which levels off the explosion spectra, in particular, the average spectrum for magnitude 5.5. This corresponds to a value of $T/\bar{Q} = 0.65$ sec, where T is travel time and $\bar{Q}$ is the average Q along the path.[5] Since most of our explosions are from a distance of 83°, the corresponding $\bar{Q}$ is about 1200, which serves to corroborate the scanty available data on mantle attenuation of P-waves.[6] When our spectra are corrected for attenuation corresponding to this value of $T/\bar{Q}$, the curves of Fig. I-7 result. In these plots, the data for frequencies below about 0.5 Hz and above 2.5 Hz are not reliable, due to signal-to-noise limitations in the original spectra.

The earthquake spectra seem quite reasonable, considering the broad population over which we have averaged, and the expected emphasis of the low frequencies with increasing magnitude is clearly shown. The spectra of presumed explosions, however, which are based on a very homogeneous population, are puzzling in two respects. One is the rather regular ripple in the spectra, particularly evident on the $m_b = 5.5$ curve and quite dramatic on a plot of energy density vs frequency. The peaks are at multiples of 0.55 Hz and suggest the weak but consistent presence of an echo or phase in the data. To match the amplitude and period of the ripple in the spectrum for $m_b = 5.5$, one requires an echo delayed by 1.8 sec whose amplitude is about 20 percent of P and in phase with it. The second puzzling point is the lack of any clear dependence of the spectral shape on magnitude or, equivalently, bomb yield. By taking Haskell's[7] spectra for 5-kton shots in a hard medium and scaling up to 40 ktons, which should correspond[8] only to $m_b = 5.5$, we actually get a good fit to all three explosion curves of Fig. I-7.

With regard to discrimination, we return to the average spectra of Fig. I-6 and observe that the greatest differences are below 1.0 Hz and above about 2.0 Hz. A study of the scatter diagrams of the log spectral amplitude vs magnitude shows, however, that some frequencies with large average differences between the spectra also have large scatter and overlap of the two populations. The performance of the original spectral ratio has been closely reproduced by averaging the log spectral amplitudes over the original high and low bands and subtracting the results. This gives a quantity called "spectral difference," which is closely related to the logarithm of the conventional spectral ratio and, when plotted vs spectral magnitude, gives [as in Fig. I-8(a)] comparable separation. The earthquakes shown in this figure are all shallow. By varying the spectral bands used (especially the high band) and using frequency-dependent weights in computing the averages over these bands, we have obtained similar results of equal, but not superior, discrimination performance. However, a slightly better discriminant has been obtained by treating the departures of individual spectra from the average as random noise, independent at different frequencies. By using the residuals to the straight-line fits [Eq. (I-1)] for each frequency as standard deviations for this "noise," we have implemented a generalized likelihood ratio test to separate the populations. This test involves estimating the magnitude of each event first on the bomb hypothesis and then on the quake hypothesis, and in each case computing a log likelihood function. So far, the best separation has been obtained with this procedure when it is limited to the frequency bands $0.3 \leq f \leq 0.8$ Hz and $2.0 \leq f \leq 2.3$ Hz. The result is shown in Fig. I-8(b). The separation here is not really better than that of spectral difference (or spectral ratio) below magnitude 5.0, but it shows a much more comfortable separation at larger magnitudes.

E. J. Kelly

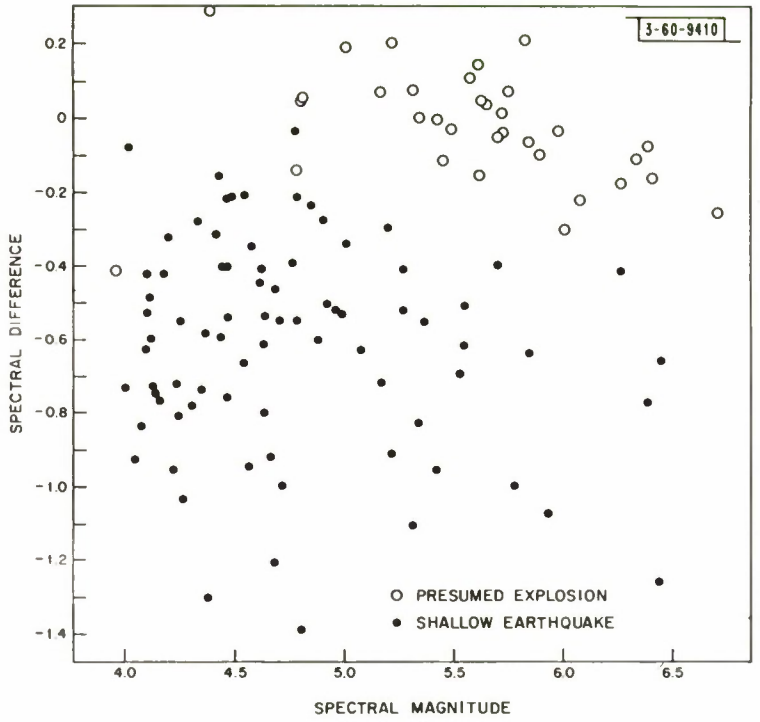

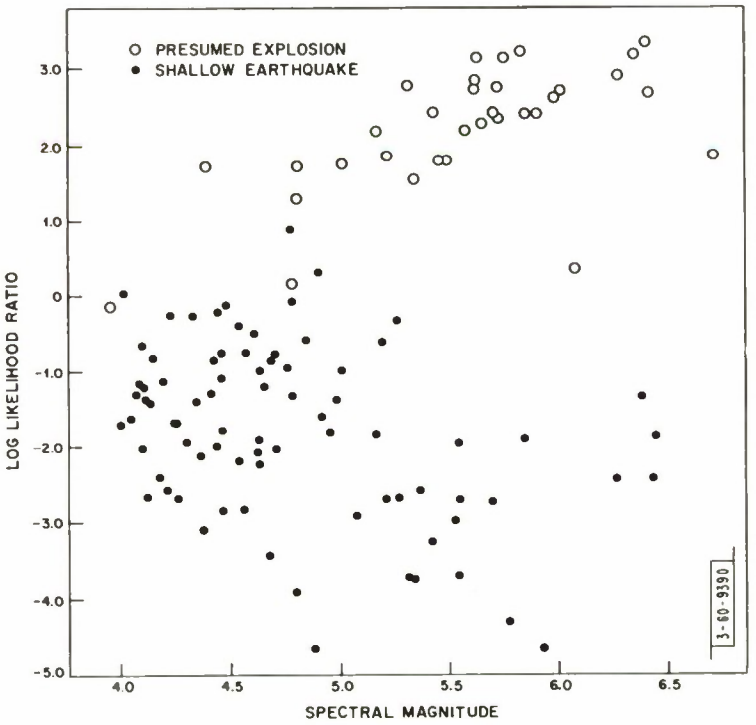

Fig. I-8. Comparison of two short-period spectrol discriminonts: (o) "spectrol difference" (roughly equivolent to old spectrol rotio criterion), ond (b) "log likelihood rotio."

C. APPLICATION OF MULTIVARIATE CLASSIFICATION METHODS

Experiments are in progress in applying several multivariate discrimination or "pattern classification" methods[9] to the seismic discrimination problem. The raw data base is a data tape containing event parameters measured at LASA on many shallow earthquakes and presumed explosions (mentioned in Sec. I-A), and about one-quarter as many events of both types measured at NORSAR. In these procedures, each event of either source type is represented as a point in N-dimensional space and a vector direction ("projection line") is sought in that space such that when the event points are projected perpendicularly on it, the best separation between classes results. Thus, there are two parts to the problem: deciding which measured parameters to consider as the N variables, and deciding which of the many available classification algorithms to use in deriving the best projection line.

In the seismic case, we have considered that the N variates may be of several types: (1) P-spectral amplitude in N frequency bands, (2) energy in N time windows starting at the initiation of P, (3) some variates from the frequency domain and the rest from the time domain, (4) mixed variables such as M_s/m_b, spectral ratio, and complexity, and (5) some variates measured at one site and some at another.

So far in this study, types (1) and (4) of these have been tested using three simple algorithms for deriving the projection line. Because of the limited event population, algorithms depending on the knowledge or assumption of some underlying probability distribution were avoided in preference to those that do not, i.e., nonparametric methods. The first method used simply employs the line connecting the centroids of the explosion and earthquake populations. This "centroid" algorithm has the disadvantage that the way in which the points in either class scatter about the centroid is not taken into account in any way; the algorithm concentrates no special attention on points lying some distance from the centroid. The second algorithm, "discriminant analysis,"[10] alleviates this defect by choosing the projection line to maximize the ratio of squared distance between projected centroids to the sum of variances of the projections within the two classes. This procedure has the disadvantage that equal attention is paid to event point projections deviating from the class mean in either direction, whether toward or away from the other class. A third procedure is being tested in which this defect is alleviated by successive iterations of the discriminant analysis algorithm in which at each iteration an event is artificially enhanced by replacing it with M identical events, where M increases from unity monotonically with the degree to which it was misclassified on the last iteration.

Several conclusions have emerged so far. The hoped-for improvements in discrimination using a large number of P-spectral components instead of just two bands, as in the spectral ratio criterion, failed to materialize – at least for LASA data. Using summed amplitudes over N = 18 equal-width frequency bands from 0.2 to 2.0 Hz gave no better performance than using as N = 2 variates the summed amplitudes over the two frequency bands 0.35 to 0.85 Hz and 1.45 to 1.95 Hz.

Adding a third variate for LASA data consisting of summed amplitudes in the 2.0- to 2.5-Hz band produced no improvement, indicating the relative inefficiency of these higher frequencies for discrimination at the Montana LASA.

Differences between NORSAR and LASA spectra appear from the limited data sample to be smaller than explosion-earthquake differences at either site. This is shown by Fig. I-9 which

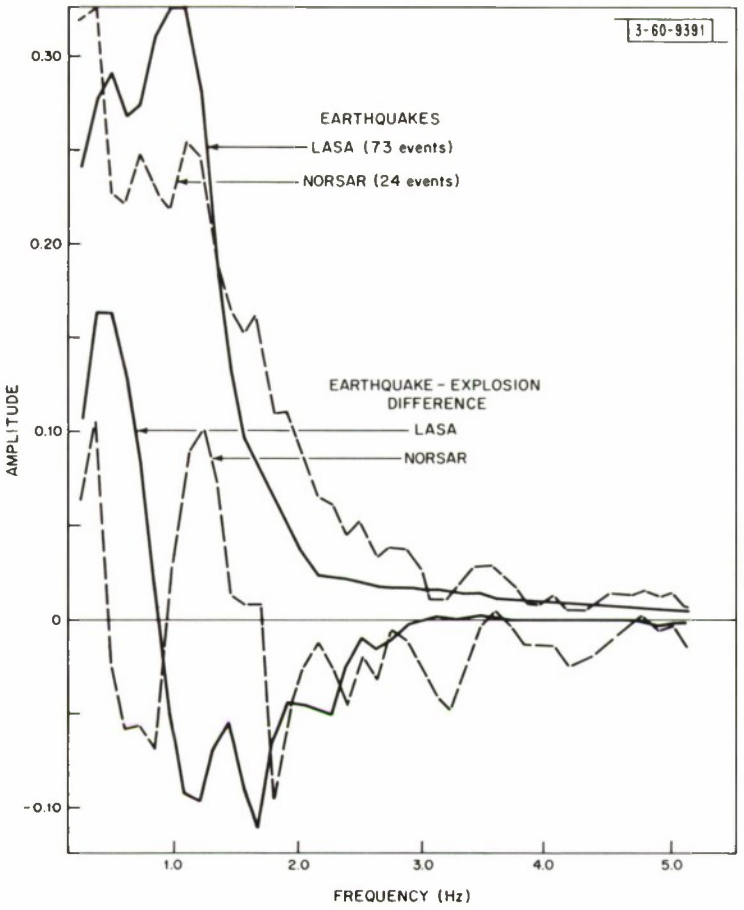

Fig. I-9. Camparisan af average spectra at LASA and NORSAR. Earthquake average spectrum far each site is average af a number af event spectra after each has been narmalized ta unit pawer. Each difference spectrum is result af subtracting a similar average aver all presumed explosians in papulatian.

gives the average spectrum (i.e., the components of the centroid read off in order of frequency) of earthquakes and the quake-bomb difference (components of a vector connecting the centroids) for the two sites. In most experiments using summed amplitudes in a given frequency band as one of the N variates, magnitude was removed as a parameter by normalizing each event spectrum to have unit power; that is, the event points all lie on the unit sphere in N-space.

When mixed discriminant criteria are used, the most effective one dominates almost completely. An example of this is shown in Fig. I-10. Positions of projected event points along a projection line using the discriminant algorithm on two variates (summed amplitudes over 0.35 to 0.85 Hz and 1.45 to 1.95 Hz as before) are plotted as the origins of arrows. Then complexity C was included as a third variate (actually C/6.0), resulting in the positions shown as the termini of the arrows. The shift in position is seen to depend on the complexity (shown for many of the events as small numbers beside the arrows), but the addition of complexity improved the source discrimination using frequency alone in no case that mattered.

Experiments on these procedures on both LASA and NORSAR data are continuing.

P. E. Green

D. VELOCITY SPECTRAL ANALYSIS (VESPA) OF P-CODA

The velocity spectral analysis program described in Sec. I-B of the last SATSR has been applied to a limited number of additional events, with results leading to two general conclusions: (1) the total observed velocity spectrum (power vs velocity) integrated over the P-arrival can be almost completely accounted for by assuming a coherent signal having a single velocity (i.e., monochromatic velocity spectrum), and (2) later arrivals, in the first minute or so after P, seem also to be monochromatic with the same velocity as P (with the exception of standard phases, such as PcP and PP).

The theoretical velocity spectra have been made more realistic by first computing the power spectrum (in frequency) for the P signal, using the output of a beam steered at the event. The parameters of a matching Gaussian power spectrum are then used in a wide-band array pattern computation[11] to obtain the theoretical velocity spectrum. The actual moveouts, including station corrections, used to form the VESPA beams are used to compute this theoretical response. Comparing this theoretical velocity spectrum (which assumes a coherent signal, i.e., one monochromatic in velocity) with measured velocity spectra, for many events using a variety of subsets of the array and weights for beamforming, excellent agreement has been observed. An example is shown in the solid and dashed curves of Fig. I-11 for an event from north of the Caspian Sea. The VESPA display for this event is shown in Fig. I-12. The phase arriving at ~20 sec after P was also processed to form a total velocity spectrum with a result which looks exactly like P. The solid and dotted curves of Fig. I-11 compare the two spectra.

A different example is shown in Fig. I-13 for a shallow shock in the Kizylkum desert in Central Kazakhstan. Here, the time-domain waveform of the beam steered at the event is compared with the VESPA display. It can be seen that many small later arrivals, discernible on the beam (but difficult to pick in single traces), appear also on the VESPA plot at the same slowness as P. In this example, there seem to be no arrivals with measurably different speeds.

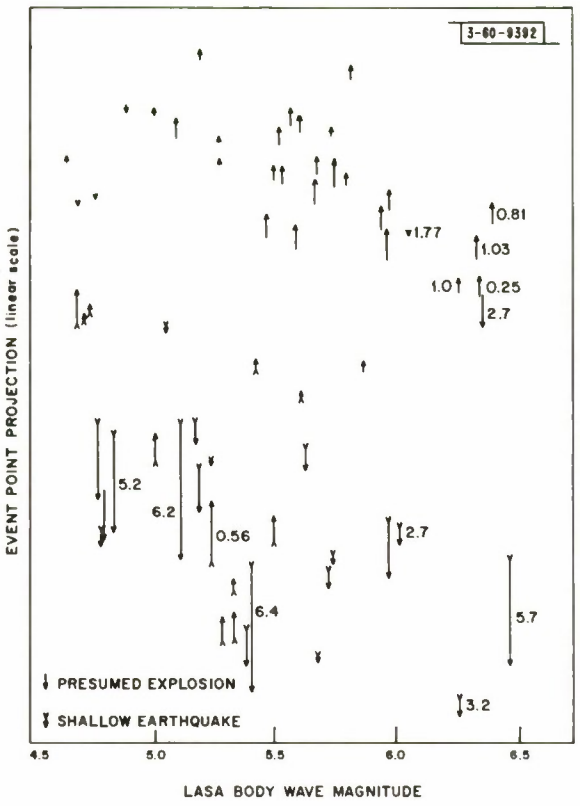

Fig. I-10. Use af multivariate discriminant algarithm ta separate presumed explosians and earthquakes. Far arraw representing each event, tail shaws result of using twa frequency damain variates (signal amplitude aver 0.35- ta 0.85-Hz and 1.45- ta 1.95-Hz bands) and head shaws result af adding ta these twa a single time-damoin measurement (complexity).

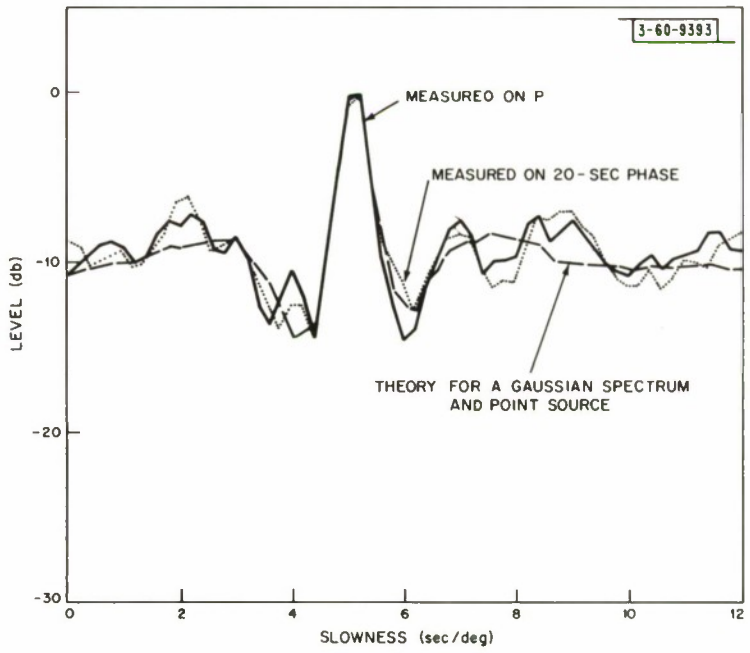

Fig. I-11. Example showing that bath P and P-coda energy orrive from a single direction.

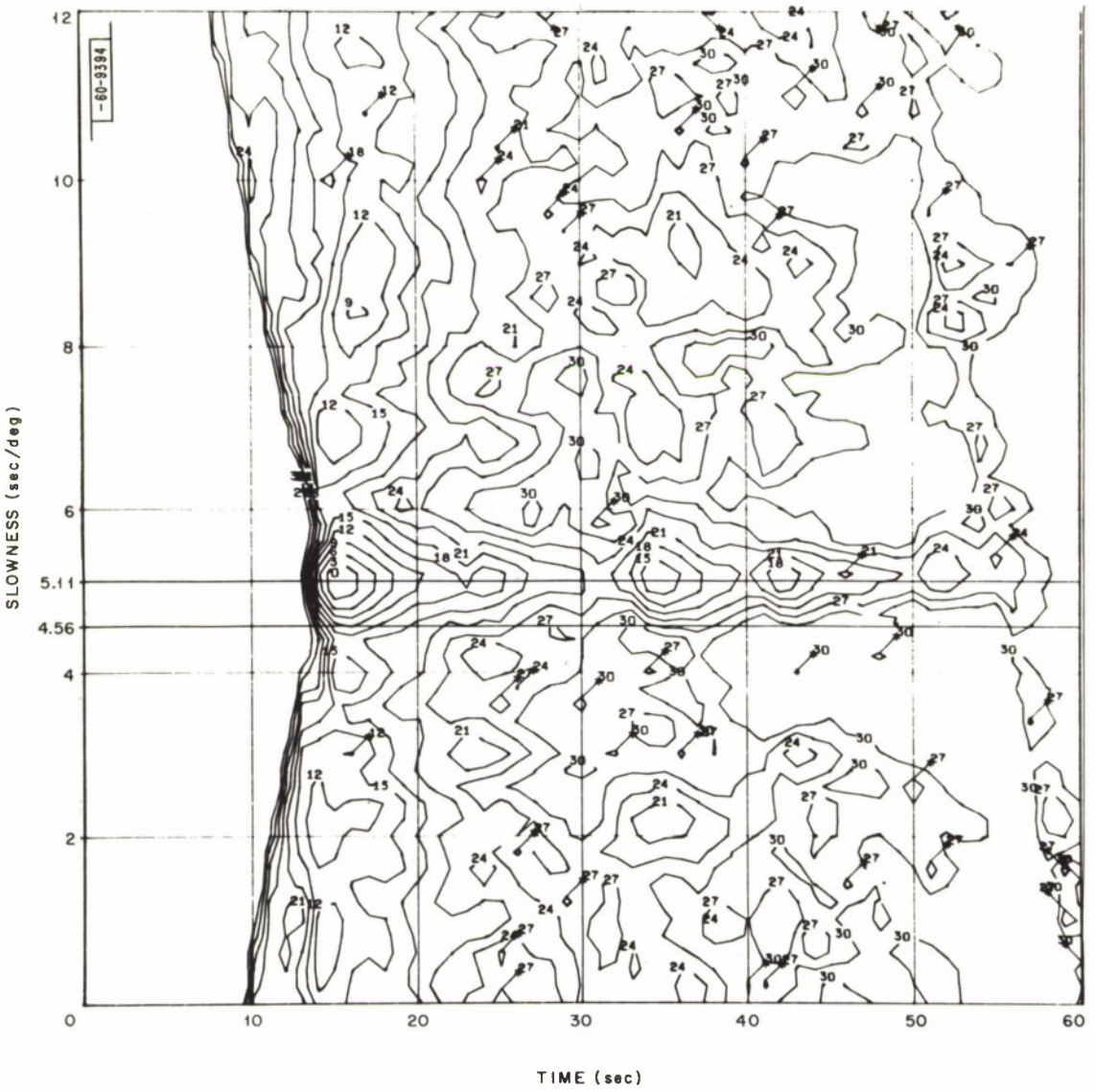

Fig. I-12. VESPA display (power vs slowness and time) for event of Fig. I-11.

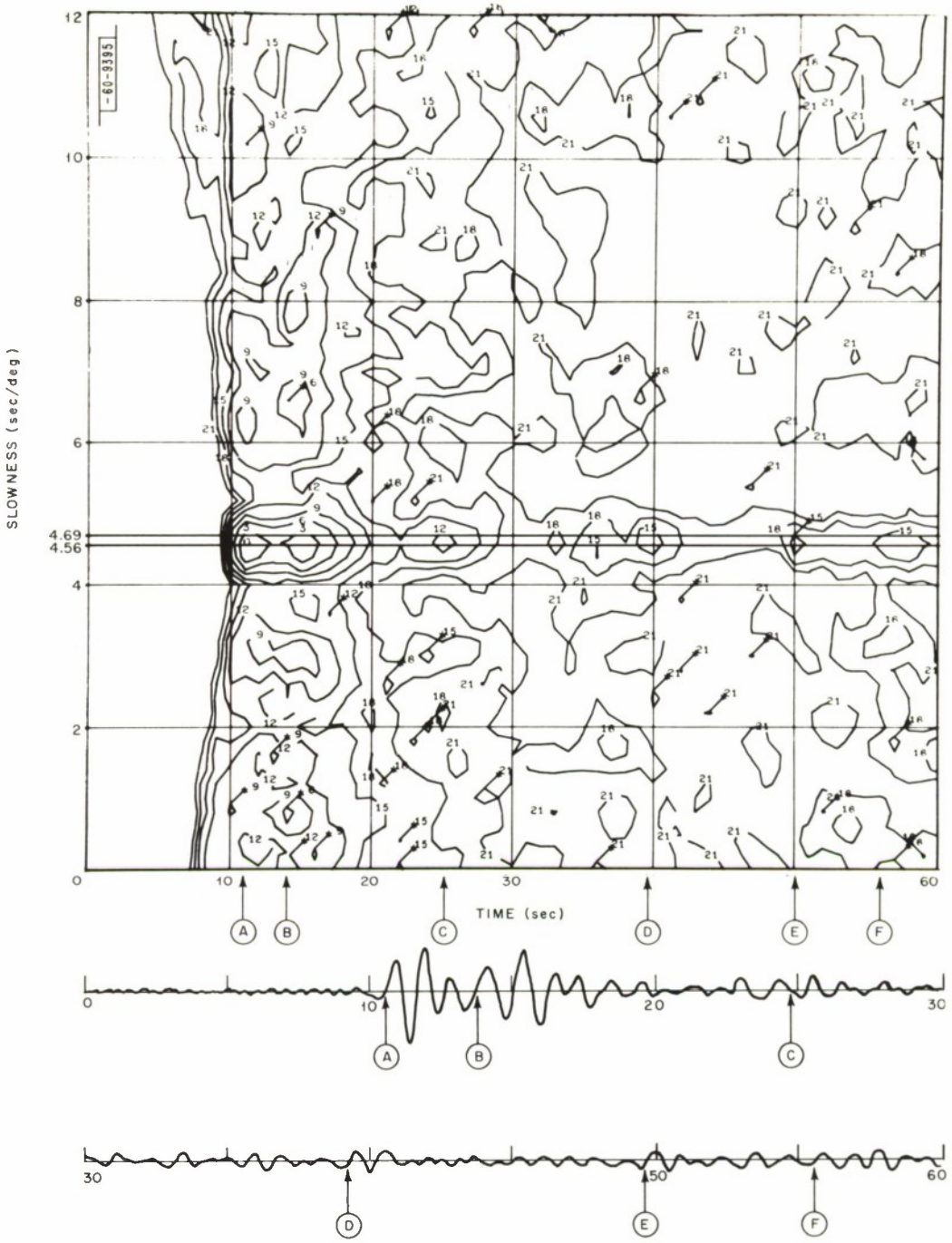

Fig. I-13. VESPA display (tap) and carrectly aimed beam waveform far an earthquake of 13 March 1968, $m_b = 5.2$.

This program is not intended to look for arrivals at angles very different from the angle of the P-arrival or at speeds corresponding to surface waves, such as might be expected for "signal-generated noise"[12] produced near the array. However, it does show that in every case examined most of the "reverberation" visible on the trace actually arrives with the same speed and direction as P.

E. J. Kelly

E. TELESEISMIC CODA GENERATION BY SCATTERING OF RAYLEIGH WAVES

An investigation has been carried out to explain the observation that underground explosions at Novaya Zemlya produce P-coda levels that are higher than for other test sites,[2] and higher than that predicted theoretically for a point source in a simple layered earth. The proposed mechanism is near-source scattering of Rayleigh waves into P-waves. The scatterers could be the island coastlines, river valleys, and other surface topographic irregularities. The proposed near-source Rayleigh-to-P scattering is in a sense the reciprocal of the near-receiver P-to-Rayleigh scattering proposed by Key[12] to explain low-velocity "signal-generated noise" effects at Eskdalemuir, Scotland.

As a measure of the observed coda level a quantity

$$W_{ob}(f) \equiv \frac{1}{30} \frac{\int_{10}^{40} S_f^2(t)\, dt}{\int_{0}^{10} S_f^2(t)\, dt}$$

giving the ratio of coda power to energy in the first 10 sec (presumably the direct P-wave) was measured and is shown in Fig. I-14. Here, $S_f(t)$ is the bandpass filtered output of the LASA beam steered to the event, where f is the center frequency of the filter. An equivalent theoretical quantity $W_t(f)$ was derived by assuming that the coda is generated by the conversion of Rayleigh waves to P-waves by scatterers located near the source. The source was modeled in two ways: (1) a harmonic explosive point source at depth h generates both P and Rayleigh waves, and (2) a harmonic explosive point source at depth h generates the P-wave while the Rayleigh waves are generated by a source of the same strength at the surface. The latter source model is justified on the basis that the nonlinear elastic deformation will reach the surface. Making certain assumptions about the scatterers,[13] using a value of scatterer density per unit surface area obtained by reference to a Novaya Zemlya map, and using a scattering efficiency (25 percent) consistent with theory,[14] we computed the curves of $W_t(f)$ shown in Fig. I-14.

Comparison of the theoretical and observed values indicates that the proposed scattering mechanism is capable of generating the observed coda levels. The scattering region for the first 50 sec of coda would be roughly a circle of radius 140 km assuming a 2.8-km/sec surface wave velocity. It is suggested that the high level of coda from Novaya Zemlya, compared with other test sites (e.g., Amchitka), may be because it has a much greater topographic relief over such an area. The large difference in coda levels relative to P at different receiving stations remains to be explained.

Further tests of this theory of coda generation by scattering would be near-source measurements of Rayleigh wave levels and the location of individual scatterers by either standard

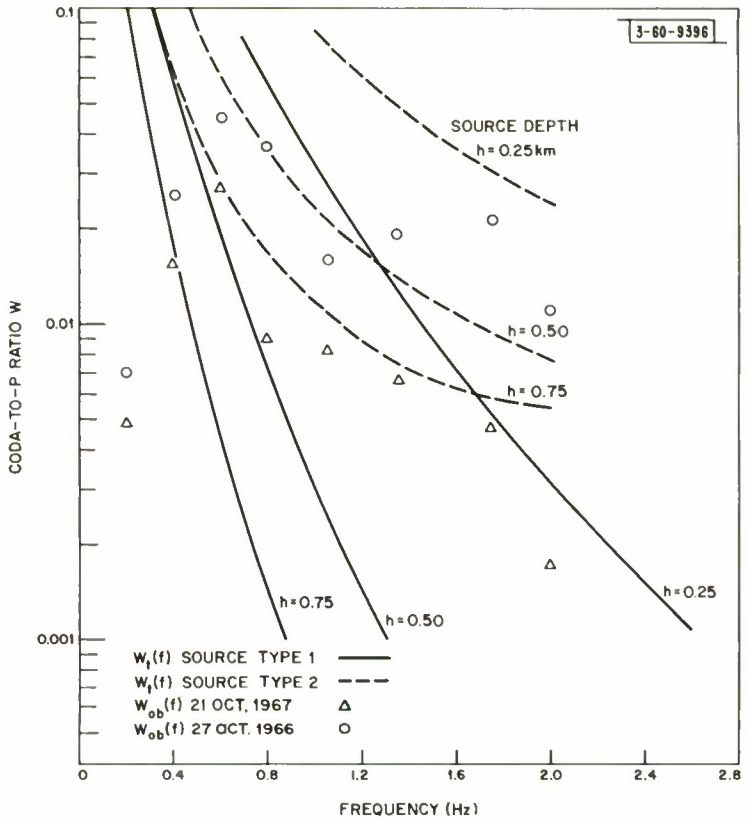

Fig. I-14. Experimental coda-to-P ratio (points) and theoretical values (lines) calculated from two models for near-source Rayleigh-to-P scattering.

epicenter location methods or beamforming using continental arrays (Sec. II-B). A report giving a more complete description of the computations is in preparation.

R. J. Greenfield

F. SURFACE WAVE DISCRIMINATION AT NORSAR

Several experiments were carried out to obtain a preliminary look at the effectiveness of surface wave discriminant techniques at NORSAR.

Surface wave magnitudes on 21 events averaged 0.3 higher at Faldalen than at the Montana LASA. Mean differences between M_s values at the three NORSAR sites used (Faldalen, Oyer, and Trysil) were found to be as much as 0.3, averaged over 12 events from the same region (western U. S. and Mexico).

The $M_s - m_b$ discriminant was applied to western U. S. and Mexican events (11 shallow earthquakes, 4 NTS explosions) and was found to provide separation for each of the two cases individually. As Liebermann and Pomeroy[15] also found, using continental North American stations only, western U. S. events appear to be anomalous, giving higher M_s for a given m_b on both explosions and earthquakes compared with other regions that have been studied.

Since the M_s vs m_b discriminant must therefore be applied to regionalized data, we considered the problem of predicting a priori whether a given region is similar to the western U. S. or to Central Asia. The anomalous behavior of the former can be either abnormally high M_s values or low m_b values.

The lowered m_b can be explained by a relative difference in the Q of the low velocity zone of the upper mantle near the source. Preliminary examination of mean spectra from different regions indicates that this effect is in operation. The enhancement of surface waves produced by earthquakes and explosions in the western U. S. relative to Central Asia can be attributed to the relaxation of a prestressed medium. According to Kim and Kisslinger,[16] the S-wave generation is enhanced by increasing the ambient stress field near the shot hole.

A recent article by Isaacs, et al.,[17] synthesizes data from many areas into a global tectonic picture. They support a continuation of an oceanic ridge from the Gulf of California along the San Andreas Fault to the west coast of Oregon and Washington. We have found that the M_s vs m_b relation of this area (11 events) is quite similar to that of the mid-Atlantic Ridge (39 events). The M_s vs m_b characteristics of a region seem to correlate well with the tectonic picture, with oceanic ridges having high M_s vs m_b values relative to island arcs for events occurring at the same depth. However, more extensive data are necessary to substantiate this hypothesis.

A report on this work is in preparation.

R. W. Ward (Geology and Geophysics Dept., M.I.T.)

REFERENCES

1. Semiannual Technical Summary Report to the Advanced Research Projects Agency on Seismic Discrimination, Lincoln Laboratory, M.I.T. (30 June 1968), Sec. I, DDC 673354.
2. E.J. Kelly, "A Study of Two Short-Period Discriminants," Technical Note 1968-8, Lincoln Laboratory, M.I.T. (12 February 1968), DDC 666701, H-875.
3. N.A. Haskell, "Total Energy and Energy Spectral Density of Elastic Wave Radiation from Propagating Faults, Part II," Bull. Seismol. Soe. Am. 56, 125 (1966).
4. K. Aki, "Scaling Law of Seismic Spectrum," J. Geophys. Res. 72, 1217 (1967).
5. L.M. Dorman, "Anelasticity and the Spectra of Body Waves," J. Geophys. Res. 73, 3877 (1968).
6. T. Asada and K. Takano, "Attenuation of Short-Period P-Waves in the Mantle," J. Phys. Earth 11, 25 (1963).
7. N.A. Haskell, "Analytic Approximation for the Elastic Radiation from a Contained Nuclear Explosion," J. Geophys. Res. 72, 2583 (1967).
8. "Seismic Methods for Monitoring Underground Explosions," Report of the International Institute for Peace and Conflict Research (SIPRI), Stockholm, 1968.
9. G. Nagy, "State of the Art in Pattern Recognition," Proc. IEEE 56, 836 (1968).
10. P.G. Hoel, Introduction to Mathematical Statistics, Third Edition (Wiley, New York, 1962), pp. 179-184.
11. Semiannual Technical Summary Report to the Advanced Research Projects Agency on Seismic Discrimination, Lincoln Laboratory, M.I.T. (30 June 1967), Sec. IV-E, DDC 657327.
12. F.A. Key, "Some Observations and Analyses of Signal-Generated Noise," Geophys. J. Roy. Astron. Soc. 15, 377 (1968).
13. K. Aki, "Analysis of Seismic Coda of Local Earthquakes as Scattered Waves," to be published in J. Geophys. Res.
14. A.J. McGarr and L.E. Alsop, "Transmission of Reflection of Rayleigh Waves at Vertical Boundaries," J. Geophys. Res. 72, 2169 (1967).
15. R.C. Liebermann and P.W. Pomeroy, "Relative Excitation of Surface Waves by Earthquakes and Underground Explosions," presented at the Magnitude Symposium, XIV General Assembly of IUGG, Zurich, Switzerland, 29 September 1967.
16. W.H. Kim and C. Kisslinger, "Model Investigation of Explosions in Prestressed Media," Geophysics 32, 633 (1967).
17. B. Isaacs, J. Oliver, and L.R. Sykes, "Seismology and the New Global Tectonics," J. Geophys. Res. 73, 5855 (1968).

II. MULTISITE EXPERIMENTS

A. DATA LIBRARY

Most of our work in the past has centered around the use of LASA data. We are now working toward the use of a worldwide network of stations. Before analysis of a network can begin, we must acquire a representative library of data and prepare a structure of computer programs and standard data formats. We have expended a considerable effort in this area, and the present status is summarized below.

Our library now contains two collections of data from networks of stations. The first consists of data from three United Kingdom arrays, the "00 NW" LRSM station (at Ringsaker, Norway), and LASA for 10 selected days during summer and fall of 1967. The long period data in this collection is limited to LASA and 00 NW, but the SP sites are well distributed around the world. The second collection consists of events recorded at LASA and NORSAR. Starting in October 1968, digital data have been requested from TFO also. LP data from both LASA and NORSAR are included for all events in this collection.

Data in both collections may be augmented by digitizing analog tapes from the LRSM stations for selected events. Data from one event have been digitized and merged from the analog tapes from eight LRSM sites and TFO, but the procedure is cumbersome and new digitizing programs are being prepared. A major problem in using data from analog tapes is accurate determination of time and sample rate (tape speed). For some studies, such as the continental array beamforming, precise absolute time is not essential, and the additional stations available from LRSM data may be very valuable.

A special epicenter location program is being written which uses starting epicenters provided by a large array and then improves the location by use of network data.

H. W. Briscoe
P. J. Connolly
R. M. Sheppard

B. CONTINENTAL ARRAYS

A computer program has been written to process the digital seismic data obtained from sensors located over an aperture of continental dimensions. At present, the data are the digitized and merged records from LRSM sites located in North America.

The purpose of the continental array program is twofold: (1) to determine the depth of an event by recognizing the arrival of the pP phase, making use of P-pP differences in velocity which are undetectable with the limited LASA aperture, and then (2) to determine the P-wave source structure of the event in the form of power vs time and source latitude and longitude (somewhat analogously to the VESPA technique described in Sec. I-D).

The program operates in the following manner. It is assumed that the epicenter, but not the depth, of the event is known, as well as the P-wave arrival times at all of the stations comprising the continental array. These times are used to bring the P-waves at the various stations into time alignment. Amplitude weights are also used to equalize gains. A beamforming operation over about 1 sec of data is then performed over the network at successive times corresponding to trial depths ranging from 10 to 200 km. The delay times used in the beamforming

operation correspond to those for pP-P (or sP-P) times and are obtained by interpolating on depth and distance in a table for these times. The power of the appropriate beam output over the appropriate 1-sec interval is computed as a function of the trial depth, and the trial depth that corresponds to the peak of these powers is then taken to be the true depth.

The computed value of depth is used in the determination of the directional structure of the source P-phase and coda. A beamforming operation over successive 5-sec intervals, starting with the P-arrival time, is performed, resulting in a plot of power vs various latitudes and longitudes about the source hypocenter at the computed depth, one contour plot for each 5-sec interval. A theoretical network beam pattern is also computed and plotted in a similar manner to provide a basis for comparison with the experimental results. The delay times used in the beamforming operation are P-times relative to the initial P-arrival and are obtained by essentially interpolating on depth and distance in a travel time table.

At the present time, the computer program has been completed and has been applied to one event.

J. Capon

III. ARRAY STUDIES

A. LARGE ARRAY EPICENTER LOCATION USING HIGH-RESOLUTION FREQUENCY-WAVENUMBER ANALYSIS

An attempt has been made to improve the epicenter location capabilities of LASA by employing the high-resolution frequency-wavenumber analysis, described in Sec. II-B of the preceding SATSR, on the short-period P-arrival. Either the conventional beamforming or the high-resolution technique can be used to generate contour plots of power vs source latitude and longitude in a manner similar to the generation of contour plots of power vs two components of horizontal wavenumber as used in microseismic noise studies (see Fig. 8 in the SATSR dated 30 June 1968). The latitude and longitude that correspond to the maximum power then yield the epicenter of the event.

The high-resolution technique was employed in conjunction with the conventional beamsplitting method, both employing station corrections. It was assumed that the conventional method was employed first to obtain an estimate of the epicenter, and thus LASA-to-epicenter azimuth and P-wave horizontal velocity, as well as the center frequency of the spectrum of the event as measured on the strongest beam waveform. The results of both the conventional and high-resolution methods are shown in Fig. III-1 for a 13 March 1968 Central Kazakh earthquake of CGS magnitude 5.2, normal depth (≈33 km), and CGS latitude and longitude 42.4 N and 66.5 E, respectively. The contours represent constant power levels in decibels relative to the peak power. Thus, the point labeled zero in each figure corresponds to the beam having the maximum power or, equivalently, the estimated epicenter. The point marked as a cross corresponds to the location given by the CGS. It is seen from Fig. III-1(a-b), that both the conventional and high-resolution methods yield about the same estimate for the epicenter, which in this case is different from the CGS estimate by about 3°. This agreement is typical of that obtained in a number of runs. However, the contours generated by the high-resolution method show a much sharper peak than the conventional method.

Because the peaks obtained by the two methods are similarly in error, there does not appear to be much (if any) advantage in the use of a high-resolution method relative to the conventional method for improving the epicenter location accuracy of LASA.

J. Capon
R. M. Sheppard

B. DIRECTION OF APPROACH OF RAYLEIGH WAVES

The high-resolution frequency-wavenumber spectrum analysis program has also been used to study the direction of approach of Rayleigh surface waves using the LASA long-period vertical array. It is known that the beating, or modulation, of the envelope is caused by multiple path propagation of the various frequency groups.[1-3] This beating phenomenon is depicted quite clearly in Fig. III-2. On this same event, the frequency-wavenumber spectrum of the Rayleigh surface wave was measured over successive 200-sec long blocks of time, and the results are shown in Figs. III-3(a) through (d). In Fig. III-3(a), it is seen that the initial 25-sec period group arrives from approximately the azimuth of the event (312°). The results in Figs. III-3(b) to (d) show the later arrivals for this same frequency group, coming from a more northerly direction.

The azimuthal angle of arrival varies from approximately 312° to 342° for a total spread in azimuth of about 30°. A 660-km path-length difference of the wave packets in Figs. III-3(a) and (b) can be inferred from the 200-sec time delay between frames and the known 3.3-km/sec group velocity at the 25-sec period. This is in a reasonably good agreement with observations reported by Evernden who measured phase velocities by eye across a tripartite array.[2,3] The use of array processing rather than visual trace examination allows, for a given aperture, a more accurate measurement of direction, and the possibility of handling simultaneous arrivals from several directions.

J. Capon

C. SHORT-PERIOD NOISE ANALYSIS USING HIGH-RESOLUTION MAPPING

Figure III-4 shows the results of applying both the conventional and high-resolution frequency-wavenumber mapping techniques to a given sample of short-period noise, as was done earlier for long-period noise (SATSR for 30 June 1968, Sec. II-B). The sensors were selected from sub-arrays in the A, B, and C rings at LASA to form a total aperture of about 36 km with 2- to 4-km minimum spacing. Measurements were made at various frequencies ranging from 0.2 to 1.5 Hz. A frequency resolution of 0.1 Hz and a record length of 6 minutes of data were used, leading to 90-percent confidence limits of ±1.2 db. Figure III-4(a-b) shows that at 0.2 Hz, the short-period noise consists of two components – a high-velocity body wave of horizontal phase velocity about 13.5 km/sec, and a low velocity surface wave at about 3.5 km/sec, as has been found previously using the conventional method of measurement.[4]

The improvement in wavenumber resolution of the high-resolution method relative to the conventional method for short-period noise does not appear to be as good as that for long-period noise. This is probably due to the lack of coherence of the short-period waves for large spatial lags, caused by the crustal inhomogeneities. Unlike the short-period waves, the long-period waves have wavelengths much longer than the dimensions of the crustal inhomogeneities.

J. Capon

REFERENCES

1. W. L. Pilant and L. Knopoff, "Observations of Multiple Seismic Events," Bull. Seismol. Soc. Am. 54, 19 (1964).
2. J. F. Evernden, "Direction of Approach of Rayleigh Waves and Related Problems, Part I," Bull. Seismol. Soc. Am. 43, 335 (1953).
3. _____, "Direction of Approach of Rayleigh Waves and Related Problems, Part II," Bull. Seismol. Soc. Am. 44, 159 (1954).
4. M. N. Toksöz and R. T. Lacoss, "Microseisms: Mode Structure and Sources," Science 159, 872 (1968).

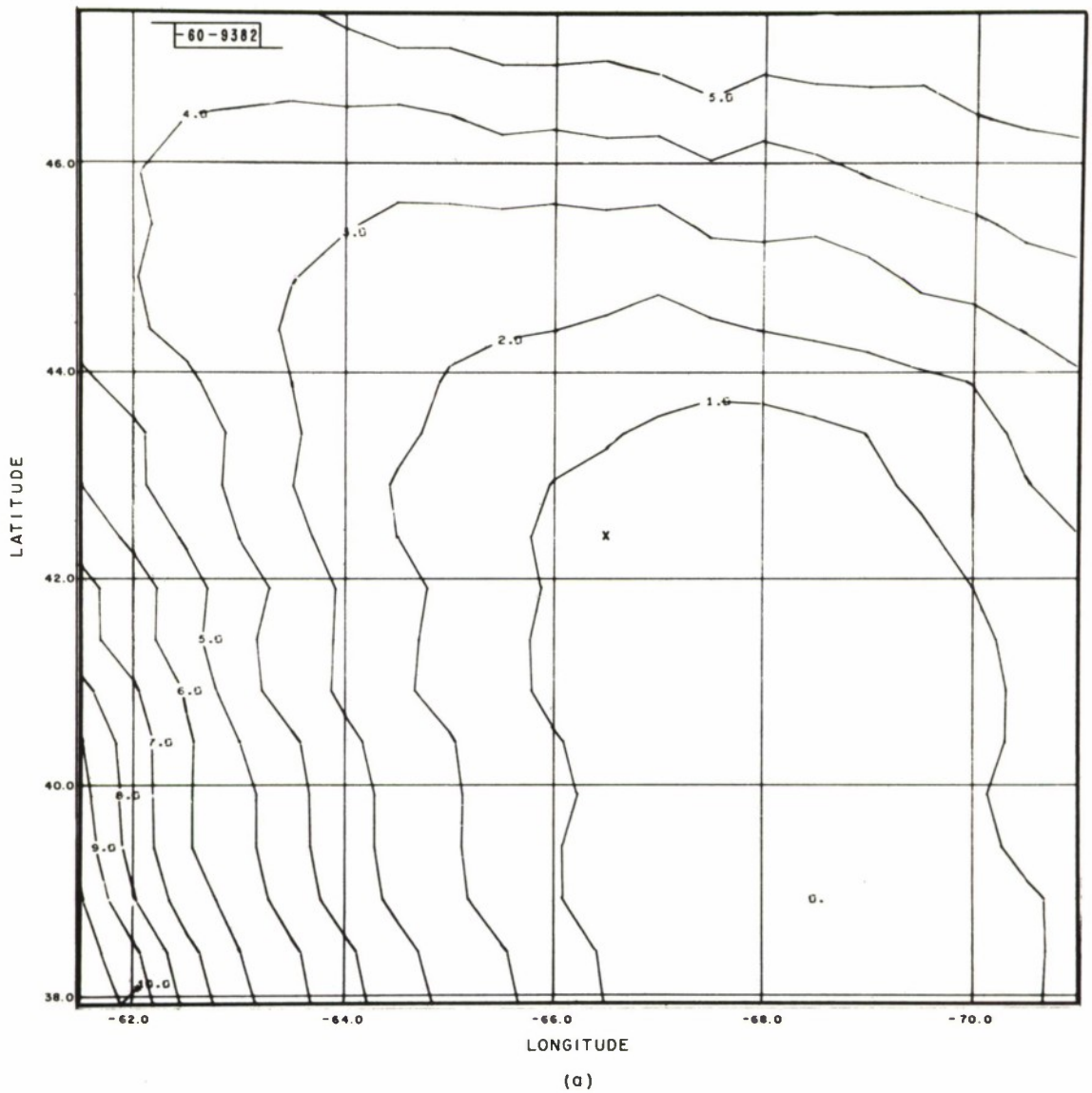

Fig. III-1. Large array epicenter lacatian using (a) canventianal beamsplitting and (b) high-resolutian mapping technique.

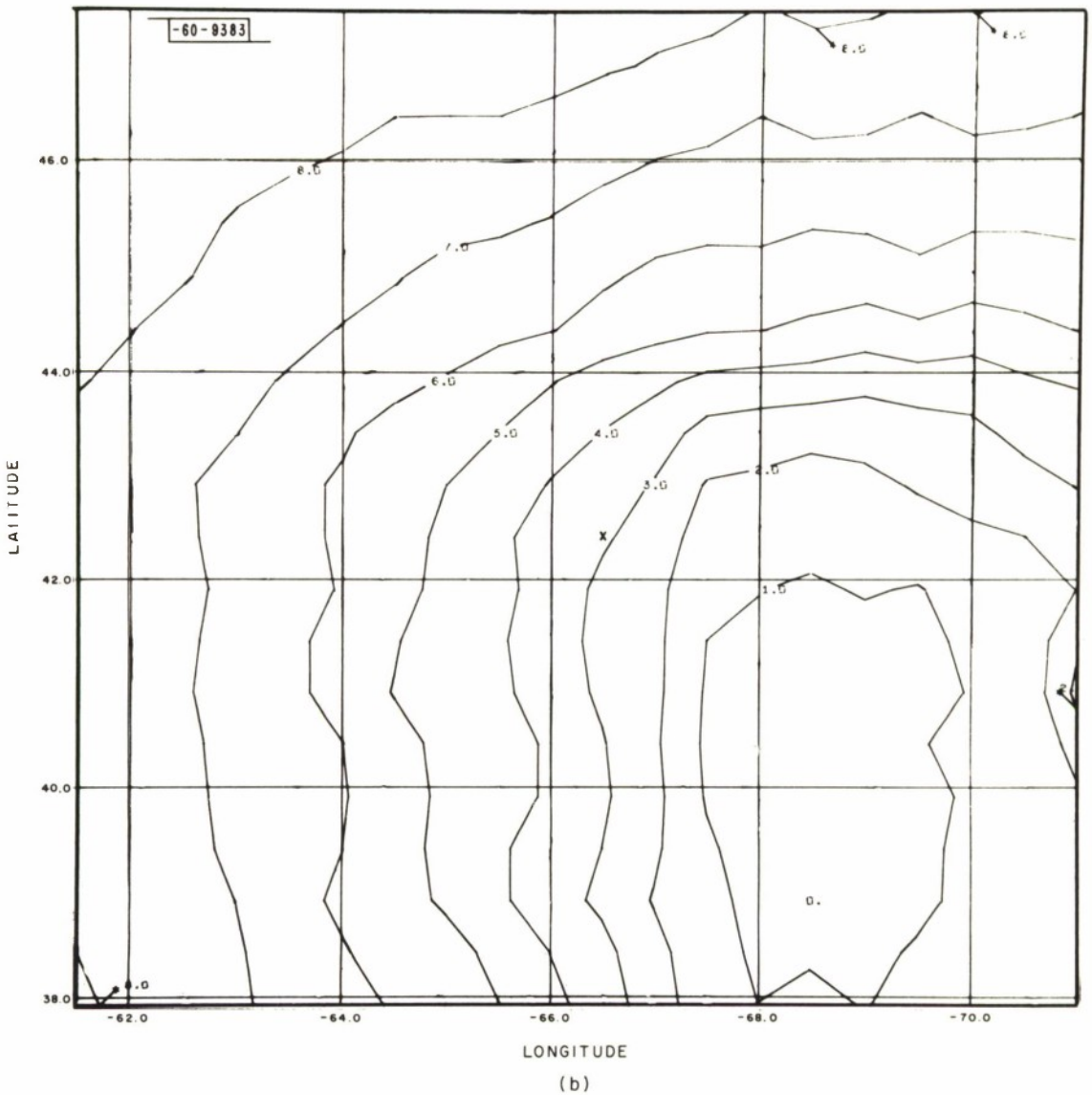

(b)

Fig. III-1. Continued.

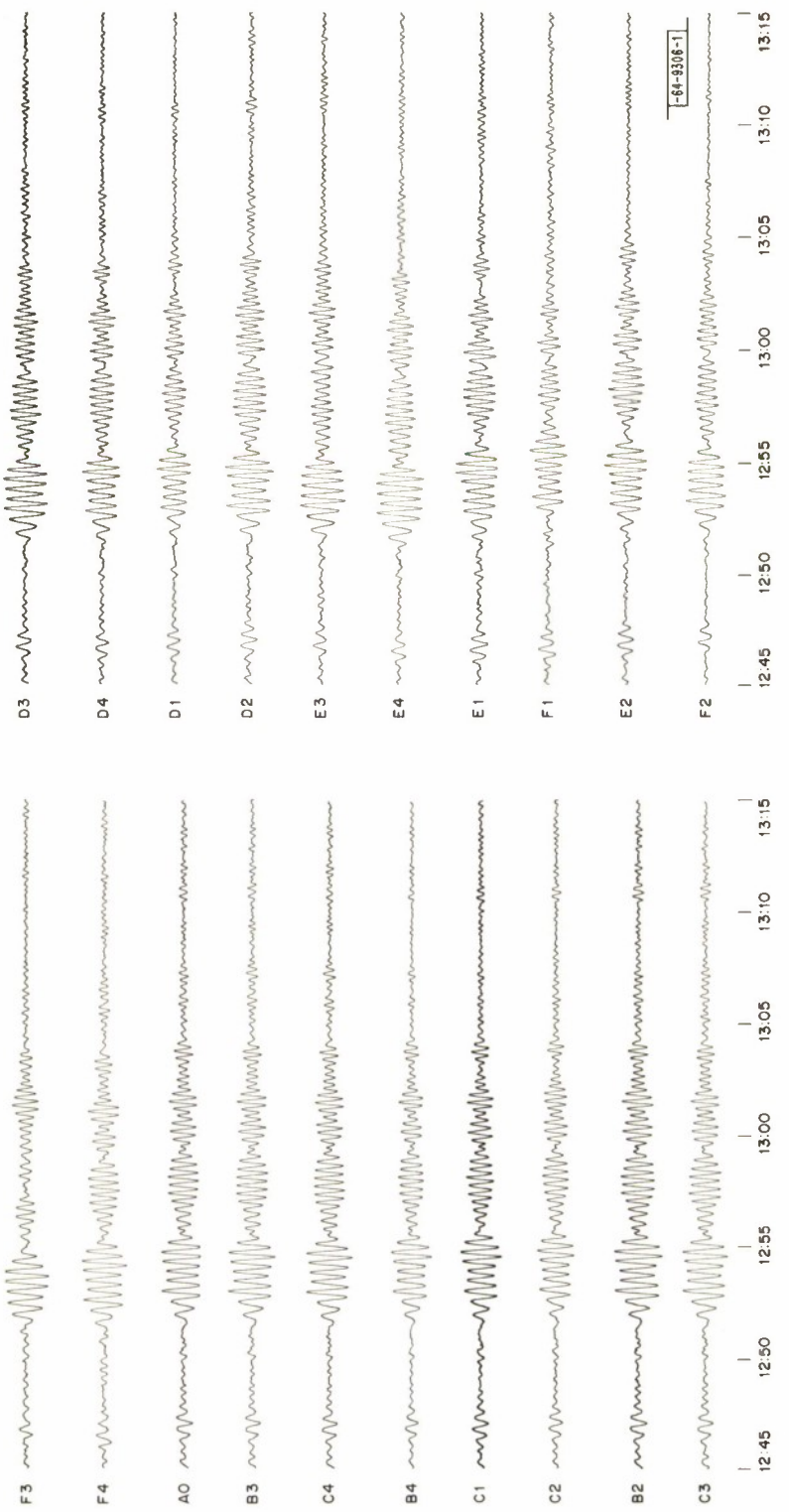

Fig. III-2. Typical LASA long-period Rayleigh waveforms (21 November 1966, Kurile Islands event).

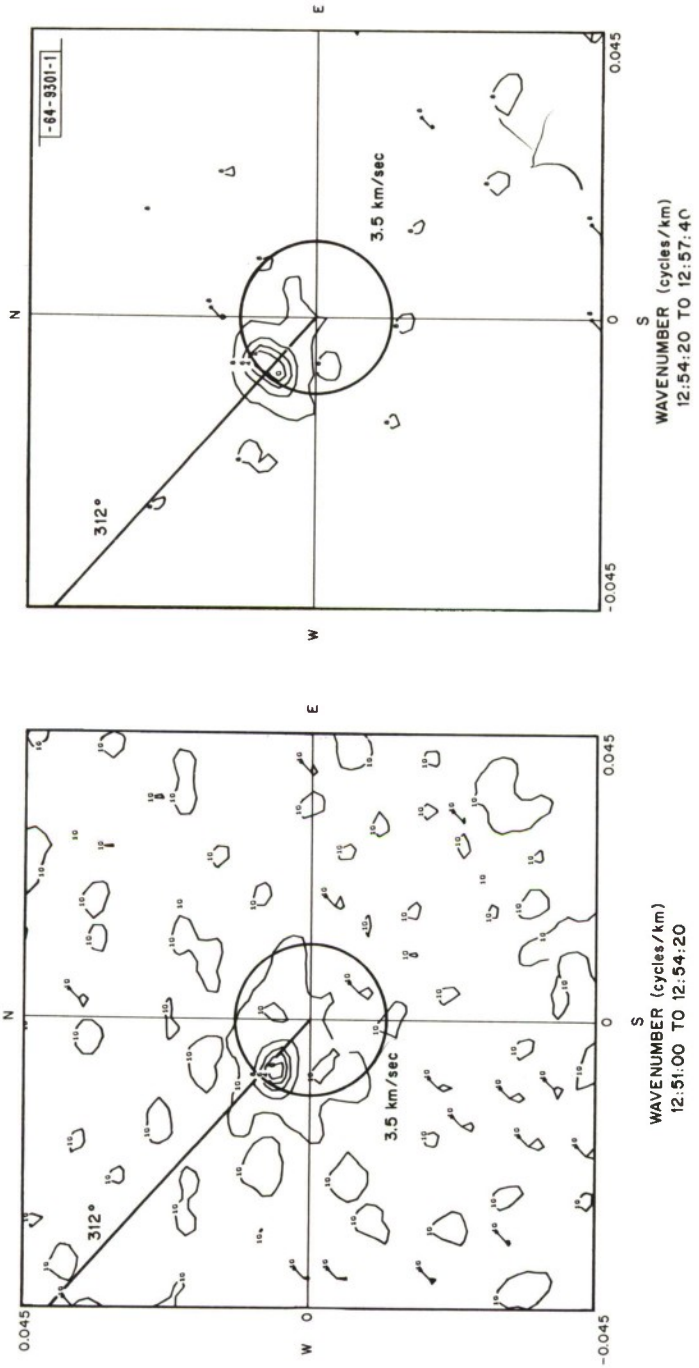

Fig. III-3(a-d). Direction of approach of Rayleigh waves of Fig. III-2 as revealed by high-resolution mapping; (a) through (d) cover successive 200-sec time windows (0.04 Hz).

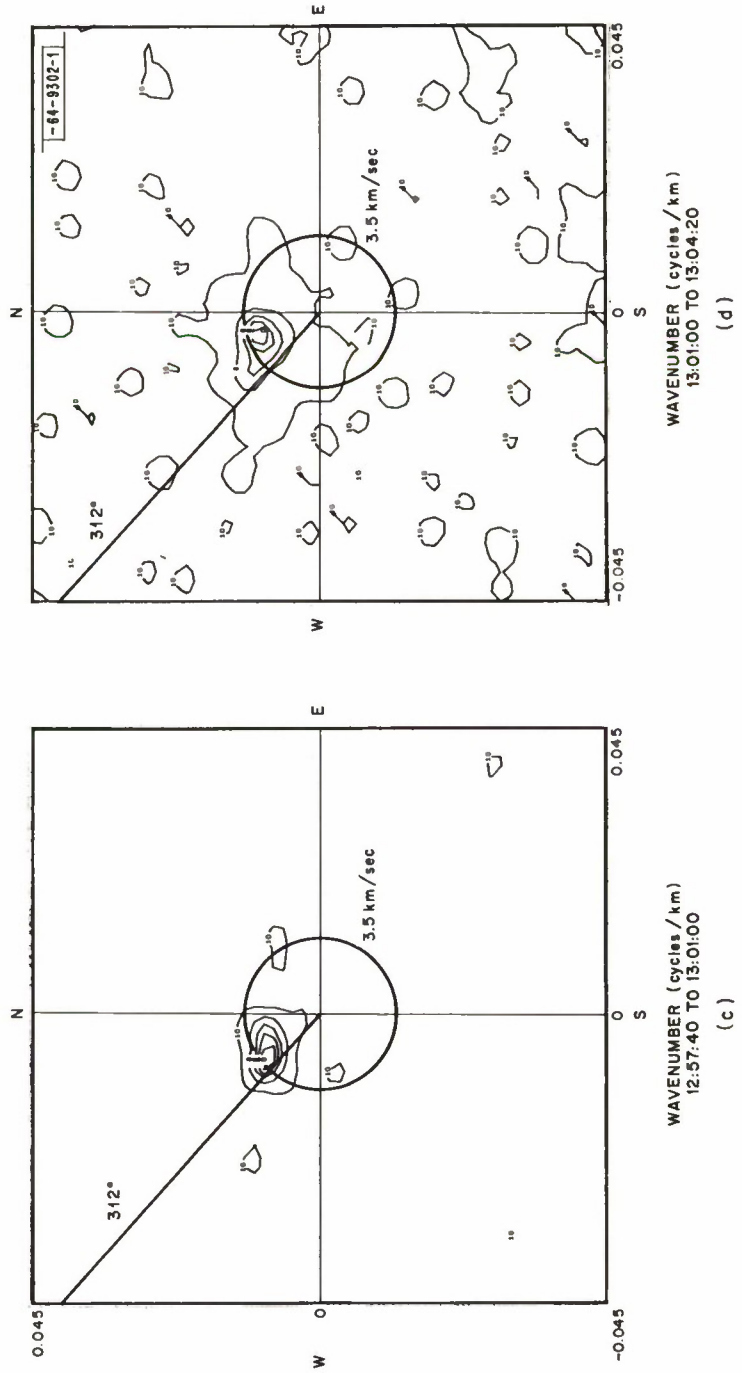

Fig. III-3. Continued.

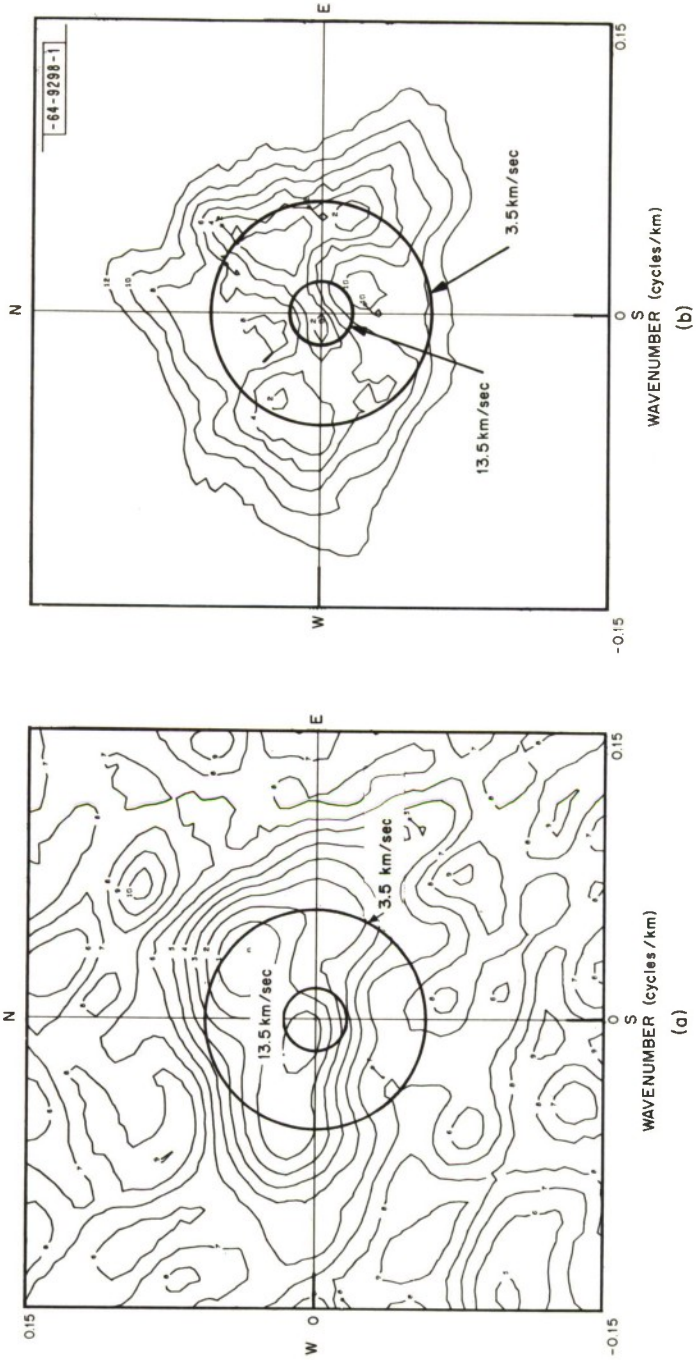

Fig. III-4. Typical example of (a) conventional and (b) high-resolution mapping technique applied to short-period noise (1 February 1967, 0803 to 0809 Z, 0.2 Hz).

IV. MISCELLANEOUS

A. PHYSICAL FACILITIES

Throughout the life of the Vela project at Lincoln Laboratory, we have taken advantage of the large reservoir of geophysical knowledge available in the Department of Geophysics at M.I.T. for discussion and consultation on experimental and theoretical aspects of the Vela problem. These discussions have played such an essential part in our technical program that approximately a year ago we began seriously to consider the possibility of physically moving the Group to the M.I.T. campus where we could work more closely with this department. As this move has progressed from an idea to a reality, we have tried to coordinate the schedules of several other changes, primarily in computer hardware and software, with the move. These changes include moving a PDP-7 from the LASA Data Center in Billings, Montana, expanding the memories in both the PDP-7 from Billings and the PDP-7 already in use in the Group, adding new display equipment to both PDP-7's, installing a magnetic drum memory to be shared by both PDP-7 computers, and installing the software system summarized in the Quarterly Letter of September 1968. Block diagrams of the hardware and software systems that we are implementing are shown in Figs. IV-1 and IV-2, respectively.

By the end of December 1968, several members of the Group had moved to the new space near the M.I.T. campus. The additional memory and the new display facilities have been added to the PDP-7 at Lincoln Laboratory, and the hardware for the modification of the computer to be moved from Billings has been delivered. The PDP-7 from Billings has been shipped to the Laboratory; this machine will be installed in the new space and modified, probably during January 1969. The machine now at Lincoln will not be moved until the second PDP-7 is working. The magnetic drum is being checked out on the machine at the Laboratory. Because of delays in installation of new telephone circuits, no schedule date for the data link from the PDP-7 to the M.I.T. Computation Center is available at this time.

The MACFLAP editor for the software system has been completed, and the Fortran IV compiler is being subcontracted. The remainder of the system programs are in the process of being coded and checked out within Group 64. Most of the software system should be completed by spring or summer of 1969.

H. W. Briscoe
P. L. Fleck

B. CALCULATED SEISMIC MAGNITUDE OF MISSILE LAUNCHES

Seismic signals from Saturn missile launches at Cape Kennedy have never been observed on the Montana LASA beams, and it was therefore considered interesting to calculate how far below the detection threshold the seismic magnitude of missile launch events should be. Results of crude (±1 magnitude unit) calculations of Saturn V body wave magnitude (m_b) and surface wave magnitude (M_S) are given at the bottom of Figs. IV-3(a) and (b), respectively. The figures show at the top cumulative daily earthquake rate vs magnitude, and at the bottom the corresponding yield of contained underground explosions based (above $m_b = 3.0$) on recently published body wave magnitude vs yield curves.[1] To plot Fig. IV-3(b), the Gutenberg-Richter relation $M_S = 1.6\, m_b + 4.0$ was used for earthquakes and the crude assumption made that a parallel straight line $M_S = 1.6\, m_b + 2.0$

M_L's for explosions (see Fig. 1 of the SATSU for 30 June 1967). The relative slopes of these readings are somewhat controversial, and there are no data around zero magnitude to resolve the question.

To calculate body wave magnitude, it was first assumed that the rocket's thrust, coupled to the ground with 20-percent efficiency, was a unit step source function applied to an infinite half-space. Then the vertical and horizontal peak amplitudes recorded on a standard 0.8-sec seismometer at several distances were calculated using the exact theoretical solution given by Pekeris.[2] The resulting local Richter magnitude for local earthquakes was roughly $M_L = \frac{1}{2}$. At distances of 600 km, M_L is close to M_S; so, assuming that the formula $M_L = 1.6\, m_b + 2.0$ is appropriate, one finds that m_b for the Saturn V is approximately −1.0. This checks roughly with an $m_b = \frac{1}{2} \pm 1$ figure derived from extrapolating measurements at 3- to 10-km distance reported by Dalins, *et al.*,[3] to teleseismic distances using Muramatsu's procedure.[4]

M_S figures for Saturn V were estimated in two ways. First, that fraction of the total explosive yield of the booster (if it were expended instantaneously) released over the first 10-sec half-period for a teleseismic Rayleigh wave was estimated to correspond to $M_S = -1\frac{1}{2}$. Second, Båth's[5] teleseismic surface wave observations of high-altitude explosions were scaled by the ratio of surface pressures during the first 10 sec, to give $M_S = -\frac{1}{2}$.

It is seen that both body and surface waves are some 60 to 80 db below the teleseismic LASA detection threshold.

P. E. Green
J. S. Derr (Geology and Geophysics Department, M.I.T.)

REFERENCES

1. D. Davies, "Seismic Methods for Monitoring Underground Explosions, An Assessment of the Status and Outlook," report by Seismic Study Group, Intern. Inst. for Peace and Conflict Res. (SIPRI), Stockholm (August 1968).

2. C. L. Pekeris, "The Seismic Surface Pulse," Proc. Nat'l. Acad. Sci. 41, 469 (1955).

3. I. Dalins, A. Eglitis, and V. McCarty, "Detection of Pure Seismic Disturbances as Generated by Large Rocket Firings," Conference paper published in Institute for Environmental Sciences Annual Technical Meeting Proceedings (San Diego, April 1966), pp. 113-121.

4. I. Muramatsu, "Correction and Remarks of the Equation of Magnitude," Zisin 19, No. 4, 282 (1966).

5. M. Båth, "Seismic Records of Explosions, Especially Nuclear Explosions, Part III," Report of Defense Research Institute (FOA), Stockholm, Division 4 (December 1962).

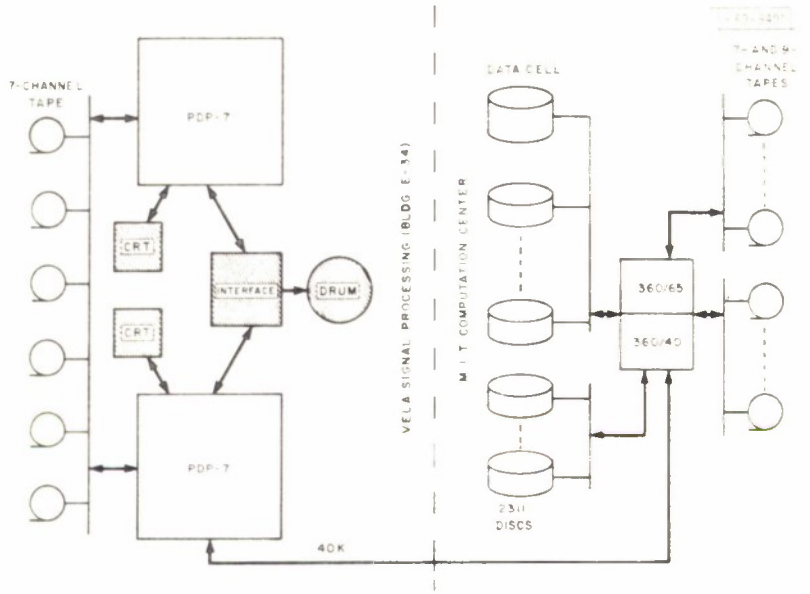

Fig. IV-1. Block diagram of computation hardware.

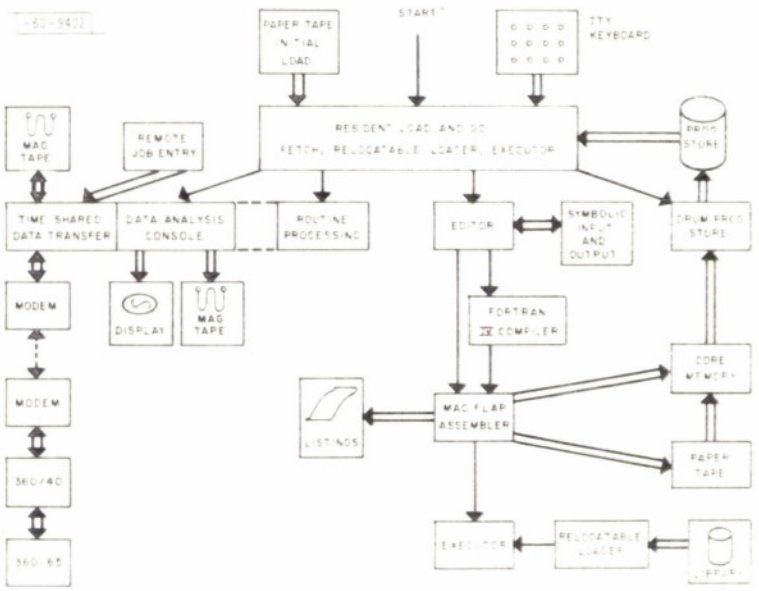

Fig. IV-2. Block diagram of PDP-7 software.

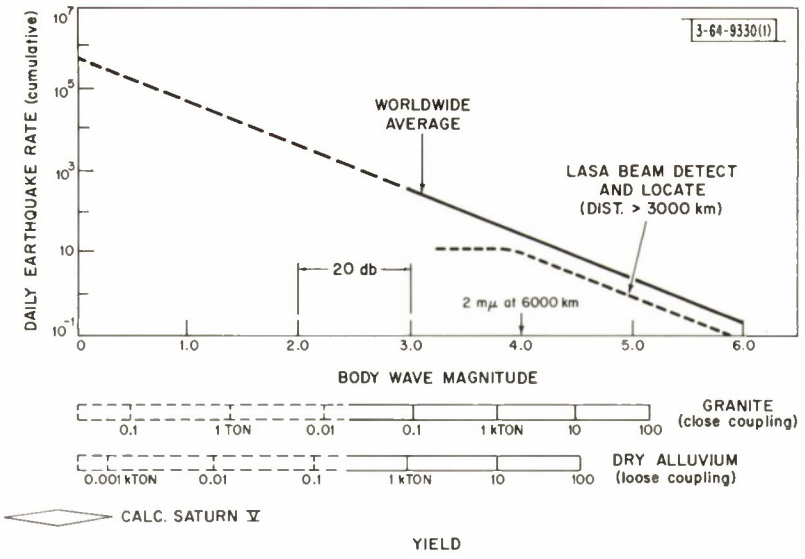

(a)

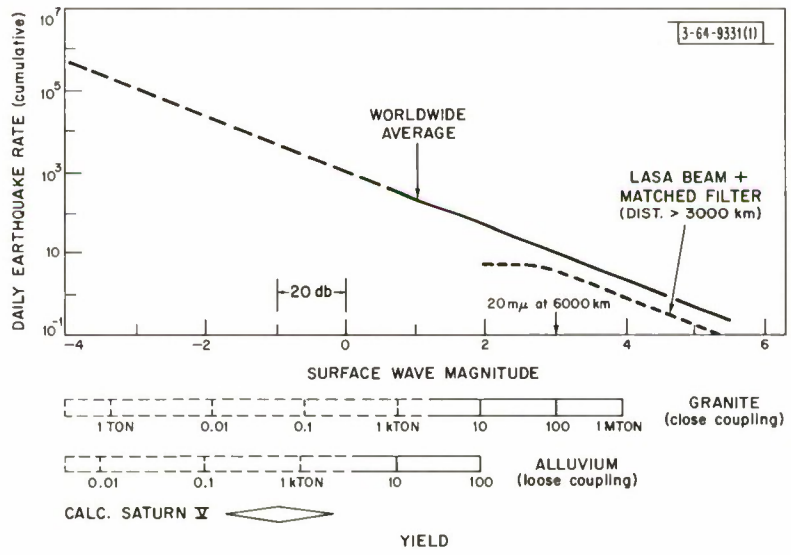

(b)

Fig. IV-3. Yield-seismicity-magnitude summary for (a) body wave magnitude, and (b) surface wave magnitude.

DOCUMENT CONTROL DATA – R&D

(Security classification of title, body of abstract and indexing annotation must be entered when the overall report is classified)

1. ORIGINATING ACTIVITY *(Corporate author)* Lincoln Laboratory, M.I.T.	2a. REPORT SECURITY CLASSIFICATION Unclassified 2b. GROUP None

3. REPORT TITLE

Semiannual Technical Summary Report to the Advanced Research Projects Agency on Seismic Discrimination

4. DESCRIPTIVE NOTES *(Type of report and inclusive dates)*

Semiannual Technical Summary Report – 1 July to 31 December 1968

5. AUTHOR(S) *(Last name, first name, initial)*

Green, Paul E.

6. REPORT DATE	7a. TOTAL NO. OF PAGES	7b. NO. OF REFS
31 December 1968	44	26

8a. CONTRACT OR GRANT NO. AF 19(628)-5167 b. PROJECT NO. ARPA Order 512 c. d.	9a. ORIGINATOR'S REPORT NUMBER(S) Semiannual Technical Summary (31 December 1968) 9b. OTHER REPORT NO(S) *(Any other numbers that may be assigned this report)* ESD-TR-68-369

10. AVAILABILITY/LIMITATION NOTICES

This document has been approved for public release and sale; its distribution is unlimited.

11. SUPPLEMENTARY NOTES	12. SPONSORING MILITARY ACTIVITY
None	Advanced Research Projects Agency, Department of Defense

13. ABSTRACT

Seismic source identification work during this reporting period has emphasized improving the ability of short-period discriminants to work at lower magnitudes, and the use of a wider variety of stations, including especially the NORSAR site in Scandinavia. During this period, plans to upgrade our signal analysis capability and at the same time move into closer proximity to the academic part of M.I.T. have reached partial fruition.

14. KEY WORDS

seismic array seismometers seismology